# Parallel generation of uniform fine droplets at hundreds of kilohertz in a flow-focusing module

David Bardin,[1] Michael R. Kendall,[1] Paul A. Dayton,[2] and Abraham P. Lee[1,a)]
[1]*Department of Biomedical Engineering, University of California, Irvine, 3406 Engineering Hall, Irvine, California 92697, USA*
[2]*Joint Department of Biomedical Engineering, The University of North Carolina and North Carolina State University, Chapel Hill, North Carolina 27599, USA*

(Received 26 April 2013; accepted 29 May 2013; published online 18 June 2013)

Droplet-based microfluidic systems enable a variety of biomedical applications from point-of-care diagnostics with third world implications, to targeted therapeutics alongside medical ultrasound, to molecular screening and genetic testing. Though these systems maintain the key advantage of precise control of the size and composition of the droplet as compared to conventional methods of production, the low rates at which droplets are produced limits translation beyond the laboratory setting. As well, previous attempts to scale up shear-based microfluidic systems focused on increasing the volumetric throughput and formed large droplets, negating many practical applications of emulsions such as site-specific therapeutics. We present the operation of a parallel module with eight flow-focusing orifices in the dripping regime of droplet formation for the generation of uniform fine droplets at rates in the hundreds of kilohertz. Elevating the capillary number to access dripping, generation of monodisperse droplets of liquid perfluoropentane in the parallel module exceeded $3.69 \times 10^5$ droplets per second, or $1.33 \times 10^9$ droplets per hour, at a mean diameter of 9.8 $\mu$m. Our microfluidic method offers a novel means to amass uniform fine droplets in practical amounts, for instance, to satisfy clinical needs, with the potential for modification to form massive amounts of more complex droplets. © *2013 AIP Publishing LLC*. [http://dx.doi.org/10.1063/1.4811276]

## I. INTRODUCTION

Droplet-based microfluidic systems present a potent platform for a variety of biomedical applications, including point-of-care diagnostics, targeted therapeutics, and high-throughput assays for biological and chemical research.[1] A subcategory of microfluidics in which two or more immiscible fluids are introduced to create discrete volumes, these systems have been studied extensively in the past decade to form simple droplets (oil-in-water or water-in-oil),[2,3] double emulsions,[4–7] irregular particles (e.g., Janus particles),[8,9] and lipid vesicles.[10] Continuous emulsion streams are formed in microfluidic systems through specialized geometries—perhaps the most common of which are co-flowing streams, cross-flowing streams, and hydrodynamic flow-focusing[11]—with a primary advantage over conventional methods being precise control of the size and composition of the emulsion.

Droplet-based microfluidic systems are, however, limited by the rate at which emulsions are produced. Generation rates for past microfluidic chips, most of which form droplets sequentially from a single droplet formation unit, rarely exceed several thousand droplets per second,[1] insufficient even to satisfy most laboratory uses, let alone clinical or industrial applications. Additionally, problematic for applications requiring small emulsions, seldom have past generation chips formed droplets in the diameter range of 10 $\mu$m or less.[1] To date, only a handful of parallelized systems using microfluidic geometries have been reported, with the key issue being

a)Email: aplee@uci.edu. Telephone: +1 949 824-9691. Fax: +1 949 824-1727.

 

that parallelization presents difficulties in flow control and fabrication complexity, demonstrated by Barbier *et al.*,[12] Li *et al.*,[13] and Mulligan and Rothstein.[14] Barbier *et al.*[12] observed strong coupling in two parallel T-junctions, with complex dynamic behavior manifesting in synchronization, quasiperiodicity, and chaos. Monodisperse emulsions were formed only in the synchronous regime. Li *et al.*[13] parallelized four flow-focusing devices and observed weak coupling between devices with identical designs, leading to the slight broadening of the distribution of droplet sizes. Mulligan and Rothstein[14] observed variation across six parallel flow-focusing generators, due to design complexities and inconsistencies in channel heights and widths, though production was monodisperse within individual droplet generators. Moreover, edge effects of the inlet manifolds had a significant effect on droplet radii in the outermost devices. More sophisticated, large parallel systems to increase the volume flow rate of the dispersed phase (i.e., the volumetric production rate, as opposed to the generation rate) have been reported by Nisisako and Torii,[15] Zeng *et al.*,[16] and Romanowsky *et al.*[17] Nisisako and Torii[15] designed a large-scale module with 256 cross-flowing droplet-formation units arranged circularly, producing droplets with a mean diameter of 96.4 $\mu$m, at a dispersed phase throughput of 320 ml $h^{-1}$. Zeng *et al.*[16] used a microfabricated emulsion generator array containing 96 channels to generate up to $3.4 \times 10^6$ droplets $h^{-1}$, or ~944 droplets $s^{-1}$, with an average diameter of 162.3 $\mu$m. Romanowsky *et al.*[17] incorporated up to 15 dropmaker units in a two-dimensional array supplied by separate levels of large distribution/collection channels. Production of single-core double emulsions, having an outer diameter of ~150 $\mu$m, exceeded 1 kg per day or 54 ml $h^{-1}$ dispersed phases, with coefficients of variation (CV) less than 6% (sampled from 8 of the 15 dropmaker units). Each of these shear-based systems succeeded in the aim of a parallel system, in that each system increased the throughput by increasing the number of channels. However, using large microfluidic geometries to accommodate high amounts of the droplet phase (i.e., to push the volumetric throughput) resulted in droplets much too large for many practical applications of emulsions, including site-specific therapeutics and next generation sequencing.

In contrast, microchannel emulsification (MCE) has emerged as a promising technique to generate many uniform fine droplets (diameter ~10 $\mu$m or less). MCE chips use microchannel arrays with a terrace to drive the dispersed phase into the gentle continuous phase flow; spontaneous droplet formation thereby depends only on the dispersed phase flow and the geometry of the device. The works of Kobayashi *et al.*[18–20] nicely illustrate this technique. Soybean oil droplets of 31-32 $\mu$m in diameter and a CV of 9%-10% were produced, in a silicon straight-through microchannel plate with 211248 channels, at a throughput capacity of 20-30 ml $h^{-1}$.[18] This maximum flow rate of the to-be-dispersed phase fell to 50 $\mu$l $h^{-1}$, though, when straight-through microchannels were downsized to form droplets below 10 $\mu$m (corresponding to a generation rate of $1.8 \times 10^4$ Hz), due to the low percentage of active channels.[19] More recently, Kobayashi *et al.*[20] presented a 60 × 60-mm MCE chip made of single-crystal silicon, containing 14 microchannel arrays and $1.2 \times 10^4$ microchannels, for mass-producing uniform fine droplets of soybean oil; throughput reached 1.5 ml $h^{-1}$, with an average droplet diameter of 10 $\mu$m. Similarly, van Dijke *et al.*[21] reported on three parallelized designs of the edge-based droplet generation mechanism; formation of 7.5 $\mu$m droplets, which occurs spontaneously along a shallow, very wide slit, reached an estimated 250 droplets per 100 $\mu$m plateau length, with a CV below 10%. Although these devices can produce a good measure of fine droplets, shear-based techniques such as flow-focusing generate a more monodisperse product, at a higher generation rate per formation unit.[1,11,21] As well, the membrane structure of MCE chips does not favor the preparation of complex droplets with controlled composition,[15] and the product quickly becomes polydisperse above a critical working range of the dispersed phase flow.[18,21]

Despite being an area of active research, shear-based microfluidic scale-up lacks a system capable of competing with MCE chips in generating, in mass amount, droplets of diameter ~10 $\mu$m or less. To be practical for applications requiring fine droplets, and in particular for clinical applications requiring many millions of droplets for intravenous or intra-arterial administration, parallel systems must be designed not with a mind for volumetric throughput, but instead for minimum droplet size and maximizing the generation frequency. We achieve this

aim by first parallelizing our flow-focusing droplet generator then modulating the fluid dynamics to induce dripping, a tipstreaming mode of droplet formation.

In this study, we present a shear-based multi-array microfluidic module and method of operation (i.e., the dripping regime) for the generation of uniform fine droplets at rates in the hundreds of kilohertz. Our multilevel, parallel module arranges eight flow-focusing units with expanding nozzle geometry in a circle with a common outlet. By increasing the capillary number—based on the flow rate of the continuous phase—we access the dripping regime of droplet breakup, thereby affording control over droplet formation to the ratio of the flows and the total flow rate (as opposed to in the traditional geometry-controlled mode, wherein droplet size is constrained by the minimum feature size in the device).[22,23] Generation of monodisperse droplets of liquid perfluoropentane exceeded $3.69 \times 10^5$ Hz at a mean diameter of 9.8 $\mu$m. By scaling up in the dripping regime, we offer a novel means of generating massive amounts of uniform fine droplets $\sim$10 $\mu$m in diameter from shear-based devices. In terms of droplet size and generation frequency—appropriate metrics for applications requiring fine emulsions, rather than volumetric throughput—our system performs on par with the most current microchannel emulsification systems and betters past shear-based scale-up systems by one to two orders of magnitude. And compared to MCE systems, our shear-based system lends itself to modification to produce more complex droplets and higher-order emulsions. Combining parallelization with a tipstreaming mode of droplet formation enables us to massively accumulate droplets of diameter $\sim$10 $\mu$m or less, suitable for clinical *in vivo* therapeutics.

## II. MATERIALS AND METHODS

### A. Solutions

Suitable fluids were chosen to form emulsions in the dripping regime at moderate, i.e., convenient, flow rates, though it should be noted that we have observed similar phenomena in initial investigations using other fluid combinations, such as triacetin oil in aqueous glycerol solution and DI water in light mineral oil, albeit under varying flow conditions. Here, we chose liquid perfluoropentane dispersed in lipid solution for comparison to previous work in a single-channel device,[23] to emphasize the benefit of parallelization in terms of generation rate. The lipid phase[23,24] consists of an aqueous solution of glycerol mixed with the stabilizing lipids DSPC (1,2-distearoyl-*sn*-glycero-3-phosphocholine, Avanti Polar Lipids) and DSPE-PEG2000 (1,2-distearoyl-sn-glycero-3-phosphoethanolamine-N-[methoxy(polyethylene glycol)-2000], Avanti Polar Lipids). DSPC and DSPE-PEG2000 were combined at 5 mg and 1.96 mg in a glass vial and dissolved in chloroform ($CHCl_3$, Sigma). Chloroform was evaporated and the vial placed in a vacuum chamber for half an hour to ensure a complete dry. Five milliliters of ultra-pure water was added, and the mixture sonicated at room temperature for 20 min in order to disperse lipid molecules. Combined with an additional 1 ml of ultra-pure water, 4 ml of glycerol (Sigma), and 1 ml of nonionic surfactant (Pluronic F-68, Sigma), the solution was placed on mild vortex for 1 min and sonicated a second time for 10 min for ensure complete mixture. Liquid perfluoropentane (dodecafluoropentane, $C_5F_{12}$, FluoroMed) served as the dispersed phase.

### B. Module design

To demonstrate parallel generation of fine liquid perfluoropentane droplets in the dripping regime, we adapted our multi-array microfluidic module for the scaled-up production of dual-layer microbubbles.[25] To instead produce droplets and to accommodate the elevated flow rates and pressures required of dripping, the current module consists of two levels of PDMS on a glass substrate and occupies a reduced footprint. Continuous lipid and dispersed perfluoropentane phases are infused in the bottom level, shown in Figure 1, in order to maximize bond strength at the inlets (as the strength of bonding between PDMS and glass far exceeds that between PDMS and PDMS). Three bifurcations in the bottom level split the lipid phase into eight ($2^3$) channels, equal to the number of droplet formation units; vertical through-holes connect these channels to the functional array in the top level of the module. Perfluoropentane first

passes through a vertical through-hole, and then bifurcates into a like eight channels. Figure 2 shows a schematic for the top-level array, which features a radial design having an inner diameter of 14.6 mm between opposing orifices. To apportion all fluids equally among all orifices in the array, we follow the design criteria that the flow resistance in the channels must be much less than the flow resistance through the flow-focusing regions.[17] Extended distribution channels (i.e., resistors) increase resistance in the perfluoropentane flow just prior to each orifice; as well, small channels prior to and post each orifice (38 $\mu$m and 30 $\mu$m wide, respectively) and orifices $8.1 \pm 1.4$ $\mu$m in width further increase resistance through each formation unit relative to along the larger distribution channels. As an added benefit, these extended distribution channels also serve to minimize crosstalk among orifices and make generation less susceptible to fluid disruptions by neighboring production and sources.[12,26] The distribution channels and orifices were narrowed to their current dimensions in order to increase the local velocities of the fluid flows, particularly of the continuous phase, at the flow-focusing regions, thereby elevating the capillary number to induce the geometry-controlled to dripping regime transition. The dependence of the mode of droplet formation on the capillary number—$\mathrm{Ca} = \eta V/\gamma_{\mathrm{EQ}}$, where $\eta$ is the viscosity and $V$ is the superficial velocity of the continuous phase, and $\gamma_{\mathrm{EQ}}$ is the equilibrium surface tension between the continuous and dispersed phases—has been shown previously in studies utilizing flow-focusing devices.[22,23]

### C. Microfabrication and assembly

Standard soft lithography techniques[27] were used to fabricate the microfluidic chips, forming negative channels by pouring PDMS over 25 $\mu$m thick positive SU8-25 (MicroChem) master molds. Devices were designed as vector-based geometries in Illustrator (Adobe) and printed at 20000 DPI by CAD/Art Services. A consistent 10:1 mixture of PDMS (Sylgard 184, Dow Corning) prepolymer to curing agent was used for both levels of the module and cured overnight in a 70 °C temperature-controlled dry oven. Levels were peeled from the hard masters in a laminar flow chamber, and inlets and outlet were punched using a blunt 18 G needle. First, a soda lime glass slide was cleaned with isopropyl alcohol and bonded to the bottom level of the module after 90 s in air plasma at 250 milliTorr and 200 W (Harrick Plasma). This pair and the top level were then plasma treated and bonded using transitional spacers for alignment (Figures 2 and 3). The transitional spacers were formed from thin plastic sheets; two strips were cut to ~0.6 cm in width and folded five times to form a zigzag pattern ~3.5 cm in length with ~2 cm handle. After the second round of air plasma, these spacers were placed along the length of the bottom level at opposing edges to create a gap of ~0.5 cm between this level and the top. Then, the top level was aligned to the bottom with minimal effect to the surface activation due to the folds; removal of the transitional spacers allowed surfaces to touch and bonding to occur. To maintain hydrophilicity of the channels, 0.05% polyvinyl alcohol solution was injected into the outlet of the module and allowed to wick; the module was dried in a vacuum chamber then baked overnight at 70 °C to complete the surface treatment.

To accommodate the elevated flows required for droplet formation in the dripping regime, all sides of the multilayer module were coated with a 5:1 ratio of PDMS prepolymer to curing agent prior to baking the module overnight at 70 °C, shown in Figure 3. At this ratio, the PDMS cures to become a hard rubber sealant, essentially minimizing weak points that otherwise cause blowouts in the PDMS-PDMS bond between the top and bottom levels. Sans sealant, these blowouts—which form between PDMS levels, allowing fluid to escape a distribution channel along a path of minimal resistance to the edge of the module—tend to arise as the total flow rate is ramped up, preventing stable access to dripping.

### D. General equipment and procedures

The microfluidic module was mounted on an inverted microscope (IX71, Olympus) and external fluidic connections were made via flexible tubing (Tygon, Sigma). The lipid phase was pumped at a constant volumetric flow rate using a digitally controlled syringe pump (Pico Plus, Harvard Apparatus). Liquid perfluoropentane was supplied using a homemade pressure pumping

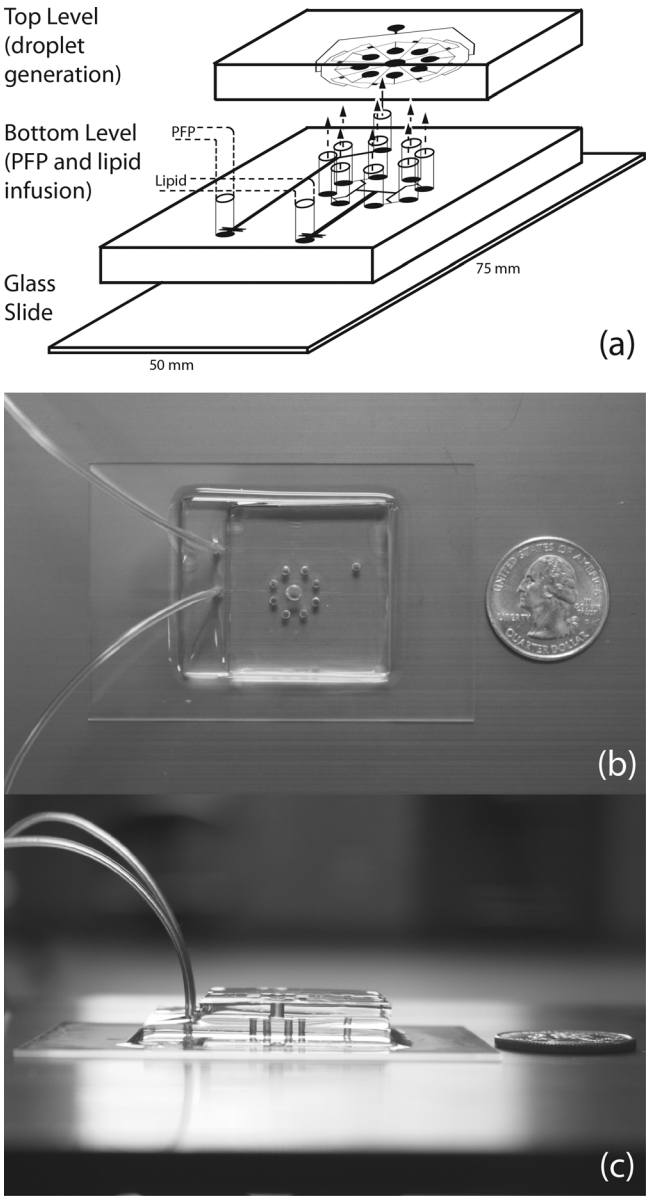


FIG. 1. The multilevel microfluidic module for the generation of uniform fine droplets. (a) A schematic view of the two levels of the module. Geometric channels in each level bifurcate and equally distribute lipid solution and liquid perfluoropentane to the eight hydrodynamic flow-focusing units of the radial array. (b) Overhead view of the assembled PDMS module relative to a quarter. (c) Side view of the module relative to the quarter.

system controlled by a Swagelok analytic regulator with a Swagelok 100 PSI gauge, to minimize fluctuations in the dispersed phase flow and eliminate the buildup of pressure in the channels. A high-speed camera (V310 Phantom, Vision Research) was used to record videos of droplet generation at the flow-focusing region of each orifice (eight videos per flow condition). At each flow condition, IMAGE J (NIH) was used to determine the generation rate $f$ (droplets $s^{-1}$, or Hz) and mean droplet diameter $D$ ($\mu$m) and variance $s^2$ for each orifice; more specific, mean droplet diameter was back calculated from area measurements of thousands of droplets taken optically from recorded images. The pooled generation rate $f_p$ for the module was calculated as the sum of individual generation rates, also used as weighting factors to determine the pooled droplet diameter $D_p$ as

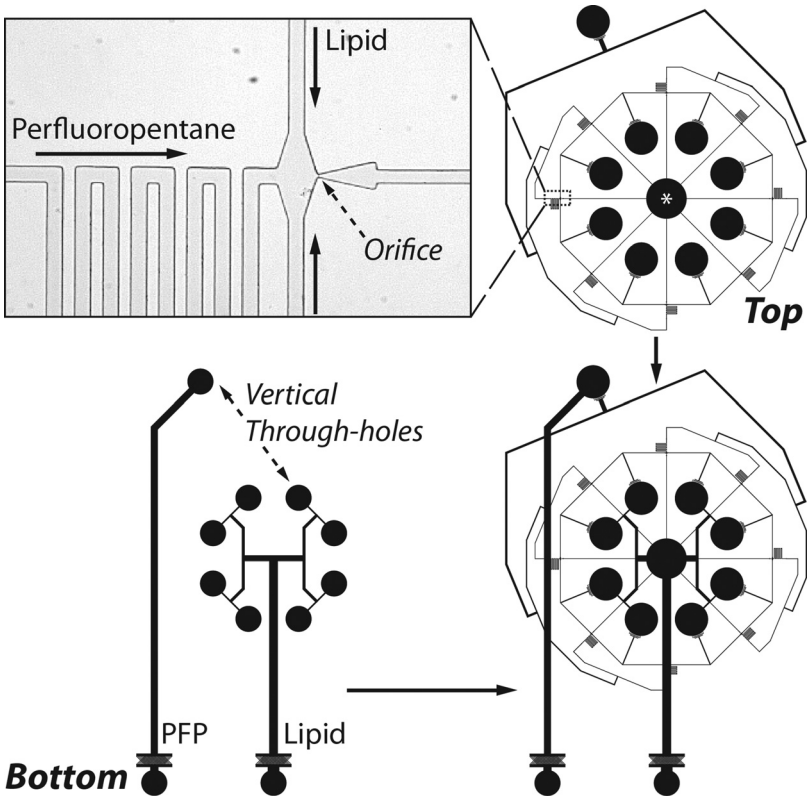


FIG. 2. Geometry of the multi-array module. Bottom and top levels are aligned using transitional spacers and bonded via air plasma treatment. Overall footprint of the module measures 20.9 × 29.9 mm. Channels are rectangular with a height of 25 $\mu$m. Droplets are generated into a central collection reservoir, denoted here by the star (*). (inset) Image of a flow-focusing region. Lipid solution and liquid perfluoropentane distribution channels measure 38 $\mu$m in width and direct flows to 8.1 ± 1.4 $\mu$m orifices, succeeded by a post-orifice channel 30 $\mu$m in width.

$$D_p = \frac{\sum_{n=1}^{8} f_n D_n}{f_p}.$$

The pooled standard deviation $s_p$ of the droplet diameter was then calculated as

$$s_p = \sqrt{\frac{\sum_{n=1}^{8} [(f_n - 1)s_n^2 + f_n D_n^2] - f_p D_p^2}{f_p - 1}}.$$

The pooled polydispersity index $\sigma_p$ at each flow condition was at last determined as

$$\sigma_p = \frac{s_p}{D_p} \times 100\%.$$

Droplets were collected in the outlet well of the module and stored at room temperature in a sealed 7 ml glass vial for viewing.

## III. RESULTS AND DISCUSSION

### A. Module operation

By increasing the volumetric flow rate of the continuous lipid phase $Q_L$ (and correspondingly, the pressure of the dispersed phase $P_P$), we elevate the capillary number—$\mathrm{Ca} = \eta V/\gamma_{EQ}$,

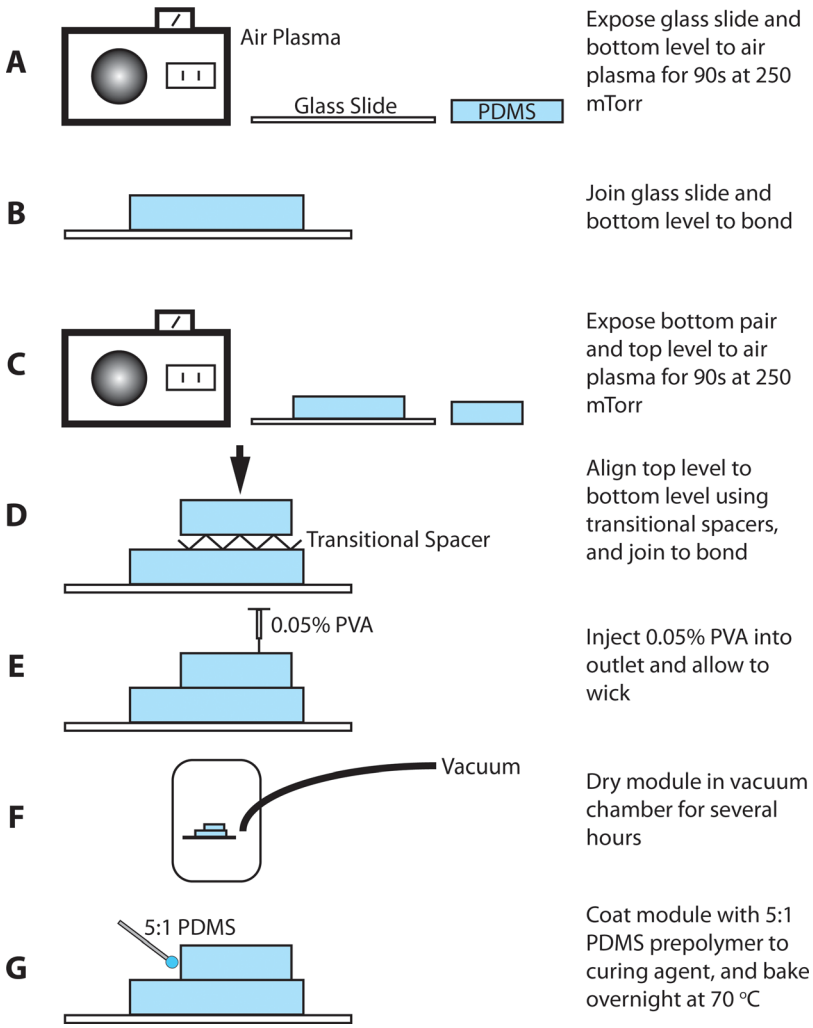


FIG. 3. Fabrication process of the parallel module. Coating the module with a 5:1 ratio of PDMS prepolymer to curing agent, and baking overnight, acts as a sealant to accommodate the elevated flows required to access the dripping regime.

where $\eta$ and $V$ are the viscosity and superficial velocity of the continuous phase, and $\gamma_{EQ}$ is the equilibrium surface tension between phases—to transition our device from geometry-controlled mode to dripping. Figure 4 demonstrates the mechanism of droplet formation for each of these regimes[22,23] via a series of images, successive in time, recorded at the flow-focusing region of a single unit. In the geometry-controlled mode ($Q_L = 100\,\mu$l min$^{-1}$, $P_P = 22.5$ PSI), droplets shear off through a protrude-and-retract mechanism:[28] the dispersed phase finger protrudes beyond the orifice constriction and experiences a high shear pinch from the sidewalls, then retracts. This dynamic process repeats to form each individual droplet. Our parallel module transitioned to the dripping regime at $Q_L \sim 160\,\mu$l min$^{-1}$, generally consistent with the 8× scale-up of our single-channel device.[23] In the dripping regime ($Q_L = 180\,\mu$l min$^{-1}$, $P_P = 33$ PSI), the dispersed phase tip highly narrows at a fixed location in the orifice and droplets break off due to steady[23] Rayleigh capillary instability.[22] The per-channel generation rate dramatically quickens and droplet size decreases in dripping relative to geometry-controlled.

### B. Parallel generation at hundreds of kilohertz

This study combines shear-based parallelization—with eight droplet formation units—and droplet formation in the dripping regime to generate uniform fine droplets in mass amount.

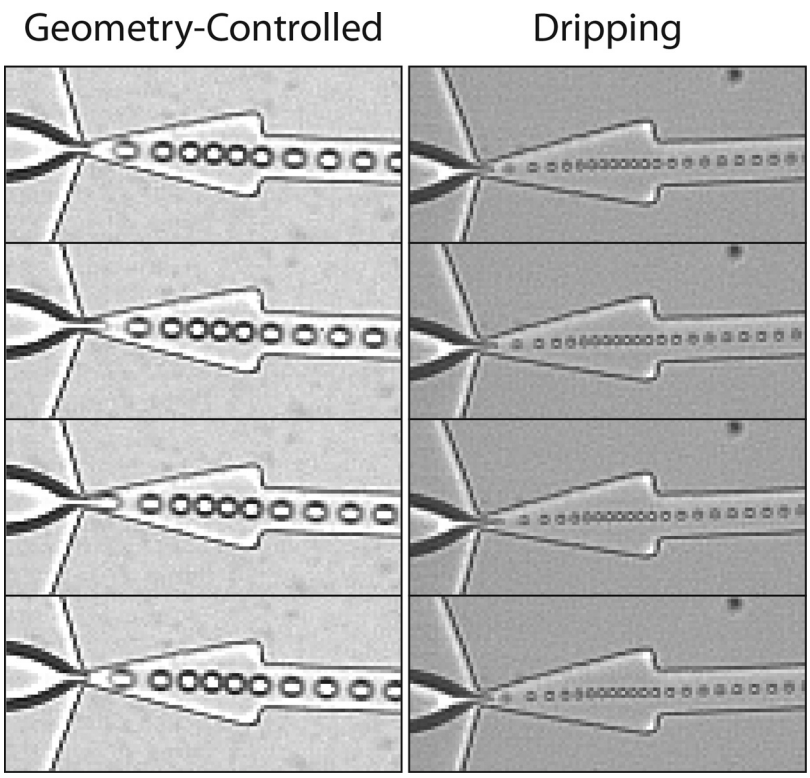


FIG. 4. Geometry-controlled vs. dripping droplet formation in the module. An elevated capillary number is necessary to transition to the dripping regime, modulated by the superficial velocity (e.g., flow rate) of the continuous lipid phase. A protrude-and-retract mechanism of the dispersed phase finger characterizes the geometry-controlled mode, whereas in dripping droplets break off the end of the dispersed phase tip, which remains at a fixed location in the orifice, due to Rayleigh capillary instability. Images are successive in time; image height is 156.25 $\mu$m.

Operated at first at the high end of the geometry-controlled mode, our multi-array flow-focusing module generated droplets of liquid perfluoropentane at $9.50 \times 10^4$ Hz with a diameter of $19.6 \pm 1.1\,\mu$m ($\sigma_p = 5.6\%$). Stable dripping formation was next realized by stepping the lipid phase flow from 100 to 180 $\mu$l min$^{-1}$ and the perfluoropentane pressure from 22.5 to 33 PSI. Generation in this sector of the dripping regime exceeded $3.69 \times 10^5$ Hz with a droplet diameter of $9.8 \pm 1.0\,\mu$m ($\sigma_p = 10.0\%$), thereby hitting our target diameter at super high speed.

To isolate the effect of parallelization on the generation rate, we compare the current module to a single-channel device forming droplets $\sim 10\,\mu$m in diameter. In a past article, we reported the formation of lipid perfluoropentane emulsions in a single-channel flow-focusing device operated in three consecutive regimes: geometry-controlled, dripping, and jetting.[23] In the single channel, the geometry-controlled mode to dripping transition occurred at $Q_L \sim 16\,\mu$l min$^{-1}$; at $Q_L = 18\,\mu$l min$^{-1}$, for droplets of a mean diameter of 9.7 $\mu$m, the generation rate reached $4.80 \times 10^4$ Hz. By comparison, under similar albeit scaled flow rates, the mean generation rate per channel in the parallel module reached $4.61 \times 10^4$ Hz in dripping (up from $1.19 \times 10^4$ Hz in geometry-controlled mode, Table I). The per-channel rate and droplet diameter after the transition to dripping thus correspond quite well to our prior data, indicating that the flow parameters and fluid dynamics at the flow-focusing region were preserved in the process of parallelization from a single device to eight devices on the chip.

Furthering the comparison to the single-channel device allows us to project the results of the parallel module for droplets in the 3–5 $\mu$m range, where the quickest rates were observed. At $Q_L = 18\,\mu$l min$^{-1}$ and a mean droplet diameter of 4.6 $\mu$m, droplets formed at a rate of $9.86 \times 10^4$ Hz as the ratio of the continuous phase to the dispersed phase reached a maximum, suggesting that even quicker rates and smaller droplet sizes should be accessible in the parallel module by increasing the dimensionless flow rate ratio $\varphi = Q_L/Q_P$, where $Q_P$ is the volumetric

TABLE I. Generation data for droplets of liquid perfluoropentane formed in the geometry-controlled and dripping regimes. The transition to the dripping regime occurred at a lipid phase flow $Q_L \sim 160\ \mu l\ min^{-1}$.

| | Lipid ($\mu l\ min^{-1}$) | PFP (PSI) | Rate ($s^{-1}$) | Diameter ($\mu m$) | PDI (%) |
|---|---|---|---|---|---|
| Geometry-controlled | 100 | 22.5 | 95000 | $19.6 \pm 1.1$ | 5.6 |
| Dripping | 180 | 33 | 369040 | $9.8 \pm 1.0$ | 10.0 |

flow rate ($\mu l\ min^{-1}$) of the dispersed perfluoropentane phase. Our experiments confirm this suggestion at individual orifices, though generation became somewhat unstable across all eight orifices of the array. Projecting across eight stable channels of a parallel module, generation should approach 1 MHz for droplets 3–5 $\mu$m in diameter. Fabrication precision currently limits this potential, as overall generation in dripping became less stable at elevated values of the flow rate ratio due to minor differences in lipid flow rate or perfluoropentane pressure at each orifice, resulting from variations in the widths of the distribution channels and orifices. For instance, by prototyping in PDMS as per convention of the field, orifice widths in the array, on the same fabricated wafer, ranged from 6.5 to 10.4 $\mu$m (on average, $8.1 \pm 1.4\ \mu m$, CV = 17.7%), affecting fluid distribution among units.

### C. Monodispersity and outliers

The multi-array module generates liquid perfluoropentane droplets with good overall monodispersity in either formation mode, as pictured in Figure 5. Operated in the dripping regime, our module generates droplets less than 10 $\mu$m in diameter at a polydispersity index below 10%. Generation is in general equivalent among orifices in the array, as no individual unit experiences less crosstalk from the array arrangement or more edge effects of the inlet manifolds than another,[14,29] a clear advantage of the radial design over two-dimensional coupling of flow-focusing devices. The size distribution of droplets is highly peaked and tightly clustered, as shown in Figure 6, indicating an overall narrow distribution. But limited fabrication precision did elevate pooled monodispersity over monodispersity of individual units: mean single-unit polydispersity indexes $\sigma_{mean}$ measured 2.3% in geometry-controlled mode and 5.6% in dripping, quite uniform and illustrative of the tight size control afforded by flow-focusing. It should be noted that pixel noise contributed to overall diameter variation, particularly in the dripping data where droplet radii are smaller, as a bent slide holder necessitated recording videos using a 10× microscope objective (standard deviations of much less than one pixel were measured).

Table II details generation in the dripping regime over all eight flow-focusing units. Unit 7 emerges as the outlier in the data, with a generation rate of $3.42 \times 10^4$ Hz compared to a mean rate of $4.78 \times 10^4$ ($\pm$ 4200) Hz among other units. The dispersed phase tip of unit 7 can be seen, in video, to extend the farthest into the orifice, and thereby we presume that this unit received the most perfluoropentane flow, due at least in part to its much wider orifice relative to other units (10.4 $\mu$m vs. $7.8 \pm 1.2\ \mu m$). This presumption is verified by calculating $Q_P = (\pi D^3/6)f$ and $\varphi$ for each channel: $Q_{P,7}$ and $\varphi_7$ are + and − two standard deviations from $Q_{P,mean}$ and $\varphi_{mean}$. Unit 7 experienced a decreased dimensionless flow rate ratio, corresponding to a slower rate and larger droplet diameter ($12.2 \pm .6\ \mu m$) as per the known dependence of dripping formation on $\varphi$.[23] Ignoring unit 7 in the data, droplet diameter in the dripping regime reduces to $9.6 \pm 0.6\ \mu m$ ($\sigma_p = 6.1\%$) and pooled monodispersity improves to on par with the monodispersity of individual units.

### D. Comparison to other microfluidic scale-up devices

While it is challenging to make a direct quantitative comparison between the systems discussed in this manuscript, as each system may use different fluids, including oil-in-water and water-in-oil droplets, and a unique setup, we can assess the performance of our module relative to others in a general sense using the figure of merit shown in Figure 7. Past shear-based

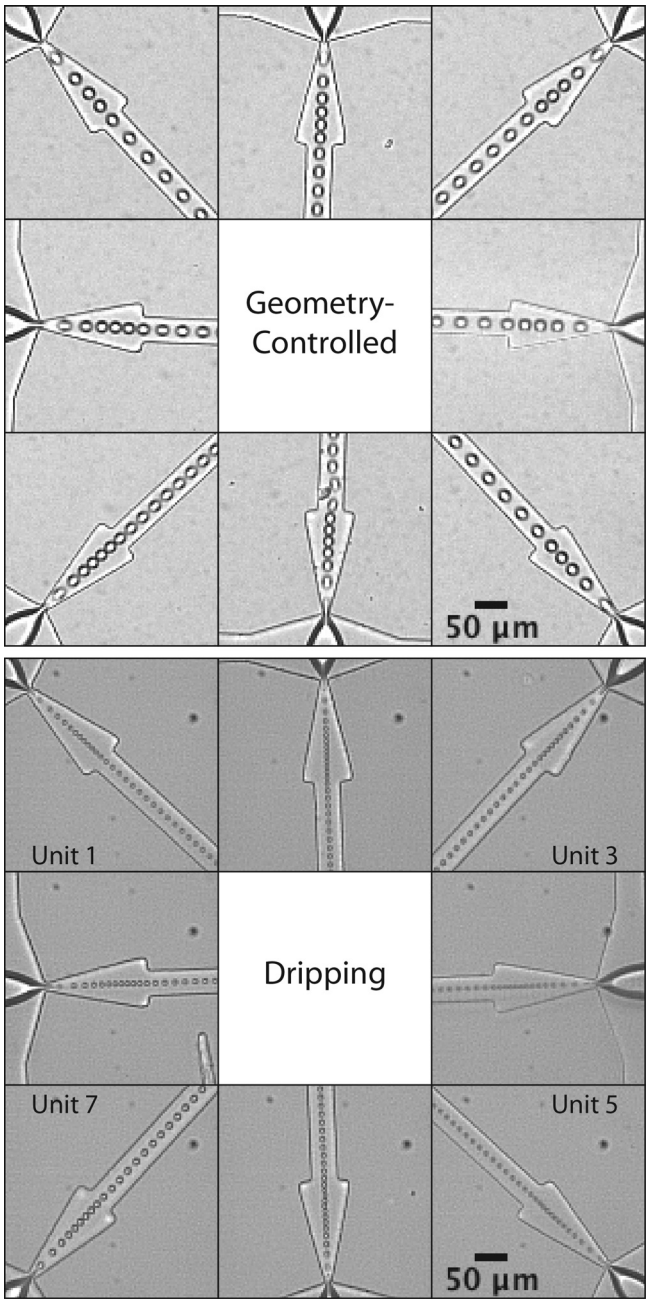


FIG. 5. Generation images for droplets of liquid perfluoropentane formed in the geometry-controlled and dripping regimes. In the dripping regime, per-channel generation rate dramatically quickens (to $4.61 \times 10^4\,s^{-1}$ per orifice, or $3.69 \times 10^5\,s^{-1}$ overall) and droplet diameter decreases (to $9.8 \pm 1.0\,\mu m$). Scale bar is $50\,\mu m$.

systems generated droplets in the range of hundreds of picoliters to nanoliters of volume, well suited for microfluidic applications in the food industry and for high-throughput screening and bioassays. At the other end of the volume spectrum, many millions of sub-picoliter droplets are required for *in vivo* therapeutics and for emerging applications in next generation sequencing (bounding the lower right region of the figure). Our shear-based module and the most current MCE chips form a cluster in this region, indicating that our module uniquely performs on par with MCE for applications of fine droplets, while maintaining the numerous advantages of shear-based generation (e.g., superior monodispersity, higher production per droplet formation unit, more straightforward fabrication).

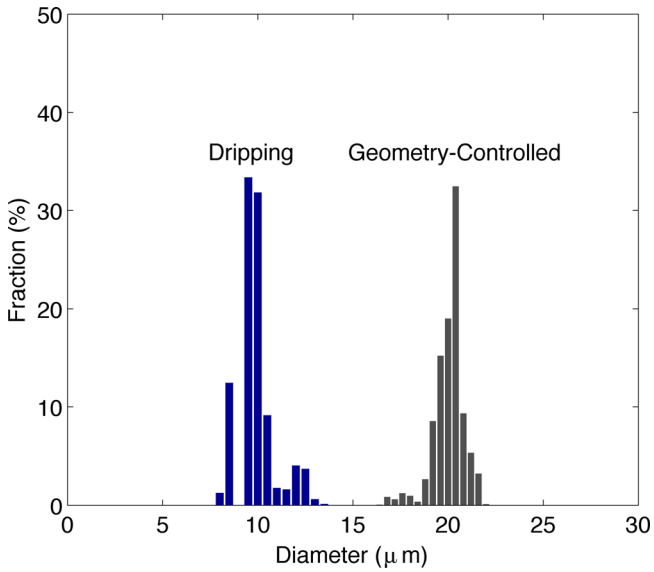


FIG. 6. Size distributions of droplets of liquid perfluoropentane in geometry-controlled mode and dripping, over the eight flow-focusing units of the multi-array module. Each unit generates quite uniform droplets. In geometry-controlled mode, $Q_L = 100\,\mu$l min$^{-1}$, $P_P = 22.5$ PSI, $D_p = 19.6 \pm 1.1\,\mu$m, $\sigma_p = 5.6\%$, $\sigma_{mean} = 2.3\%$, $f_p = 9.50 \times 10^4\,$s$^{-1}$. In dripping, $Q_L = 180\,\mu$l min$^{-1}$, $P_P = 33$ PSI, $D_p = 9.8 \pm 1.0\,\mu$m, $\sigma_p = 10.0\%$, $\sigma_{mean} = 5.6\%$, $f_p = 3.69 \times 10^5\,$s$^{-1}$. Unit 7, the outlier, contributed the peak at 12.2 $\mu$m in dripping; ignoring the data from this unit, $D_p = 9.6 \pm 0.6\,\mu$m, $\sigma_p = 6.1\%$, $\sigma_{mean} = 5.7\%$, $f_p = 3.35 \times 10^5\,$s$^{-1}$.

Volumetric throughput sees common use as a metric to measure the output of droplet-generation devices. The dispersed phase flux, volumetric throughput is determined by recording the flow rates of the dispersed phase(s) or as the product of frequency $f$ and volume $V$ ($= \pi D^3/6$). The Nisisako and Torii[15] system represents the gold standard at 320 ml h$^{-1}$ in forming droplets 96.4 $\mu$m in diameter; for multiphase droplets, Romanowsky *et al.*[17] formed double emulsions 150 $\mu$m in diameter at 54 ml h$^{-1}$. In forming much smaller droplets, our device outputs on the order of $\sim$1 ml h$^{-1}$ in terms of volumetric throughput, along with current MCE chips, despite generating droplets at higher frequency. But volumetric throughput seems an inappropriate metric to evaluate fine droplet devices due to the large positive influence of the volume term. The module presented in this work affords parallel generation of sub-picoliter droplets, down from nanoliters (a 3-log reduction). An appropriate metric for such a system should reward frequency and discount volume. As one example, we evaluate $\Omega = f/V$ as the ratio of the most positive metric (frequency of generation) to the most negative metric (droplet volume). We find that our module outputs $7.4885 \times 10^5$ droplets s$^{-1}$ pl$^{-1}$, well above the $\sim$0.5–400 range of past shear-based systems.

TABLE II. Detailed generation data for droplets of liquid perfluoropentane formed in the dripping regime ($Q_L = 180\,\mu$l min$^{-1}$, $P_P = 33$ PSI). Unit 7 emerges as the outlier in the data.

| Unit | Rate (s$^{-1}$) | Diameter ($\mu$m) | PDI (%) |
|---|---|---|---|
| 1 | 44 800 | 9.6 ± 0.5 | 5.3 |
| 2 | 54 040 | 9.2 ± 0.5 | 5.0 |
| 3 | 44 240 | 9.3 ± 0.6 | 6.7 |
| 4 | 48 720 | 9.7 ± 0.6 | 6.7 |
| 5 | 49 560 | 9.6 ± 0.6 | 5.9 |
| 6 | 51 240 | 9.6 ± 0.5 | 4.9 |
| 7 | 34 160 | 12.2 ± 0.6 | 4.8 |
| 8 | 42 280 | 9.9 ± 0.5 | 5.3 |

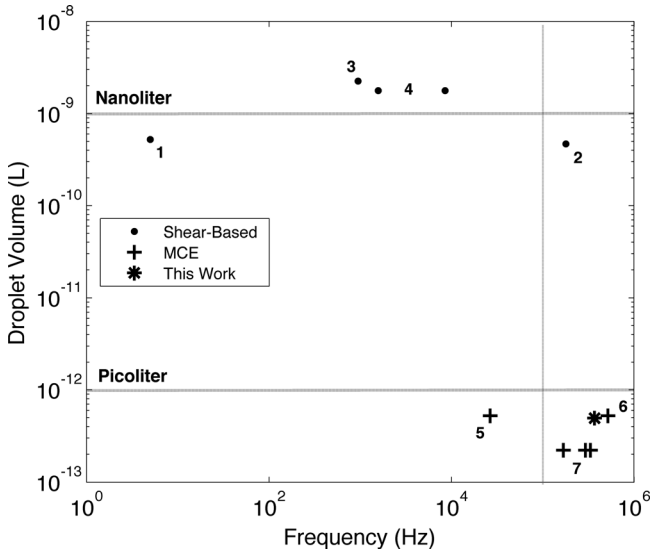


FIG. 7. Comparison of microfluidic scale-up devices using droplet volume and frequency of generation as metrics of merit. Data points 1–4 represent past shear-based systems; these systems generate droplets in the nanoliter range for applications in the food industry, high-throughput screening, and bioassays. This work forms a cluster with data points 5–7 (current MCE chips) in the sub-picoliter region for such applications as *in vivo* therapeutics and next generation sequencing. Our parallel module operated in the dripping regime generates droplets at a higher rate than past shear-based systems and reduces droplet volume by 3-log. 1—Mulligan and Rothstein (2012).[14] 2—Nisisako and Torii (2008).[15] 3—Zeng *et al.* (2010).[16] 4—Romanowsky *et al.* (2012).[17] 5—Kobayashi *et al.* (2008).[19] 6—Kobayashi *et al.* (2010).[20] 7—van Dijke *et al.* (2009).[21]

Also of note, this study consumed far less bulk fluid than previous shear-based scale-up systems in generating fine droplets. While the Nisisako and Torii[15] system and Romanowsky *et al.*[17] systems ran at continuous phase flow rates of 480 ml $h^{-1}$ and 215 ml $h^{-1}$, respectively, our multi-array module, operated in the dripping regime, required only 180 $\mu$l $min^{-1}$, or 10.8 ml $h^{-1}$, of lipid phase flow. At 9.8 $\mu$m in diameter, the droplets of liquid perfluoropentane in this study represent a ten-fold reduction or more in diameter relative to past shear-based systems (a thousand-fold reduction or more in droplet volume), with even smaller sizes achievable by increasing the dimensionless flow rate ratio, assuming improvements are made in fabrication precision.

## E. Applications

At a generation rate in excess of $3.69 \times 10^5$ droplets $s^{-1}$, or $1.33 \times 10^9$ droplets $h^{-1}$, our module amasses droplets in amounts more suitable for a laboratory or clinical setting, thus enabling many practical applications of fine droplets. Two such applications requiring many millions of droplets include site-specific therapeutics using oil-in-water droplets and next generation sequencing using water-in-oil droplets. In particular, the phase-change droplets in this study, at 9.8 $\mu$m in diameter, are amenable to intra-arterial administration[30] as gas embolotherapy (i.e., targeted vessel occlusion) agents for the treatment of various hypervascular cancers, as these droplets are stable at room temperature yet undergo rapid liquid-to-gas phase transition above a uniform acoustic or thermal activation threshold.[23] Using a more precise method to fabricate the channel geometries to be equal, the flow rate ratio could be increased in the dripping regime to stably generate smaller therapeutic droplets suitable for intravenous injection,[23,30] or sub-micron droplets for extravascular applications alongside medical ultrasound.[31] The module presented here may also serve emerging methods in next generation sequencing, with the potential to dispense single DNA templates and primer (e.g., on a bead) into several hundreds of millions of small droplets within a quarter hour, facilitating the amplification and enrichment of single DNA templates with enhanced throughput and scalability yet reduced reagent consumption.

## IV. CONCLUSION

By utilizing small channel geometries and modulating the continuous phase flow to access the dripping regime of droplet formation in a shear-based system, we demonstrated the parallel generation of uniform fine droplets of liquid perfluoropentane, $9.8 \pm 1.0\,\mu$m in diameter, in excess of $3.69 \times 10^5$ Hz. Our multi-array microfluidic module consists of two levels of distribution channels that direct continuous lipid solution and dispersed perfluoropentane to eight flow-focusing orifices arranged in a radial array. Limited fabrication precision led to an elevated pooled polydispersity, suggesting that future work should aim to improve manufacturability of the module, perhaps through the development of hot embossing in durable plastics.

## ACKNOWLEDGMENTS

Funding for this work was provided by the National Institutes of Health, Grant No. 1 RO1 EB008733-01A1. D. Bardin would like to thank NSF IGERT LifeChips Award No. DGE-0549479 for a personal graduate fellowship.

[1]S.-Y. Teh, R. Lin, L.-H. Hung, and A. P. Lee, Lab Chip **8**, 198 (2008).
[2]T. Nisisako, T. Torii, and T. Higuchi, Lab Chip **2**, 24 (2002).
[3]Y.-C. Tan, J. S. Fisher, A. I. Lee, V. Cristini, and A. P. Lee, Lab Chip **4**, 292 (2004).
[4]S. Okushima, T. Nisisako, T. Torii, and T. Higuchi, Langmuir **20**, 9905 (2004).
[5]T. Nisisako, S. Okushima, and T. Torii, Soft Matter **1**, 23 (2005).
[6]A. R. Abate and D. A. Weitz, Small **5**, 2030 (2009).
[7]A. R. Abate, J. Thiele, and D. A. Weitz, Lab Chip **11**, 253 (2011).
[8]T. Nisisako, T. Torii, T. Takahashi, and Y. Takizawa, Adv. Mater. **18**, 1152 (2006).
[9]T. Nisisako and T. Torii, Adv. Mater. **19**, 1489 (2007).
[10]S.-Y. Teh, R. Khnouf, H. Fan, and A. P. Lee, Biomicrofluidics **5**, 044113 (2011).
[11]G. F. Christopher and S. L. Anna, J. Phys. D: Appl. Phys. **40**, R319 (2007).
[12]V. Barbier, H. Willaime, P. Tabeling, and F. Jousse, Phys. Rev. E **74**, 046306 (2006).
[13]W. Li, E. W. K. Young, M. Seo, Z. Nie, P. Garstecki, C. A. Simmons, and E. Kumacheva, Soft Matter **4**, 258 (2008).
[14]M. K. Mulligan and J. P. Rothstein, Microfluid. Nanofluid. **13**, 65 (2012).
[15]T. Nisisako and T. Torii, Lab Chip **8**, 287 (2008).
[16]Y. Zeng, R. Novak, J. Shuga, M. T. Smith, and R. A. Mathies, Anal. Chem. **82**, 3183 (2010).
[17]M. B. Romanowsky, A. R. Abate, A. Rotem, C. Holtze, and D. A. Weitz, Lab Chip **12**, 802 (2012).
[18]I. Kobayashi, S. Mukataka, and M. Nakajima, Ind. Eng. Chem. Res. **44**, 5852 (2005).
[19]I. Kobayashi, T. Takano, R. Maeda, Y. Wada, K. Uemura, and M. Nakajima, Microfluid. Nanofluid. **4**, 167 (2008).
[20]I. Kobayashi, Y. Wada, K. Uemura, and M. Nakajima, Microfluid. Nanofluid. **8**, 255 (2010).
[21]K. van Dijke, G. Veldhuis, K. Schroën, and R. Boom, Lab Chip **9**, 2824 (2009).
[22]S. L. Anna and H. C. Mayer, Phys. Fluids **18**, 121512 (2006).
[23]D. Bardin, T. D. Martz, P. S. Sheeran, R. Shih, P. A. Dayton, and A. P. Lee, Lab Chip **11**, 3990 (2011).
[24]K. Hettiarachchi, S. Zhang, S. Feingold, P. A. Dayton, and A. P. Lee, Biotechnol. Prog. **25**, 938 (2009).
[25]M. R. Kendall, D. Bardin, R. Shih, P. A. Dayton, and A. P. Lee, Bubble Sci. Eng. Technol. **4**, 12 (2012).
[26]F. Jousse, G. Lian, R. Janes, and J. Melrose, Lab Chip **5**, 646 (2005).
[27]Y. Xia and G. M. Whitesides, Annu. Rev. Mater. Sci. **28**, 153 (1998).
[28]P. Garstecki, H. A. Stone, and G. M. Whitesides, Phys. Rev. Lett. **94**, 164501 (2005).
[29]M. Hashimoto, S. S. Shevkoplyas, B. Zasonska, T. Szymborski, P. Garstecki, and G. M. Whitesides, Small **4**, 1795 (2008).
[30]M. L. Fabiilli, K. J. Haworth, I. E. Sebastian, O. D. Kripfgans, P. L. Carson, and J. B. Fowlkes, Ultrasound Med. Biol. **36**, 1364 (2010).
[31]T. D. Martz, D. Bardin, P. S. Sheeran, A. P. Lee, and P. A. Dayton, Small **8**, 1876 (2012).